Kinetics of migration-driven aggregation processes on scale-free networks

Jianhong Ke,[1,2,*] Xiaoshuang Chen,[2,†] Zhenquan Lin,[1] Yizhuang Zheng,[1] and Wei Lu[2]
[1]*School of Physics and Electronic Information, Wenzhou University, Wenzhou 325027, China*
[2]*National Laboratory of Infrared Physics, Shanghai Institute of Technical Physics, Chinese Academy of Sciences, Shanghai 200083, China*

(Received 9 August 2006; published 2 November 2006)

We propose a solvable model for the migration-driven aggregate growth on completely connected scale-free networks. A reversible migration system is considered with the produce rate kernel $K(k;l|i;j)\sim k^{\mu}i^{\upsilon}(lj)^{\nu}$ or the generalized kernel $K(k;l|i;j)\sim(k^{\nu}i^{\omega}+k^{\omega}i^{\nu})(lj)^{\nu}$, at which an i-mer aggregate locating on the node with j links gains one monomer from a k-mer aggregate locating on the node with l links. It is found that the evolution behavior of the system depends crucially on the details of the rate kernel. In some cases, the aggregate size distribution approaches a scaling form and the typical size $S(t,l)$ of the aggregates locating on the nodes with l links grows infinitely with time; while in other cases, a gelation transition may emerge in the system at a finite critical time. We also introduce a simplified model, in which the aggregates independently gain or lose one monomer at the rate $I_1(k;l)=I_2(k;l)\propto k^{\omega}l^{\nu}$, and find the similar results. Most intriguingly, these models exhibit that the evolution behavior of the total distribution of the aggregates with the same size is drastically different from that for the corresponding system in normal space. We test our analytical results with the population data of all counties in the U.S. during the past century and find good agreement between the theoretical predictions and the realistic data.

DOI: 10.1103/PhysRevE.74.056102 PACS number(s): 89.75.Hc, 05.40.−a, 82.20.−w, 89.75.Da

I. INTRODUCTION

In the last few decades, considerable interest has been devoted to understanding the nonequilibrium aggregate growth, which underlies a wide variety of natural and social processes such as aerosol formation and crystal growth [1–4]. Among such investigations, a great deal of effort has been focused on the kinetics of aggregate growth through the binary coalescence mechanism, $A_i+A_j\rightarrow A_{i+j}$, namely, the aggregates A_i and A_j can bond spontaneously to form a larger aggregate A_{i+j} [5–9]. Here, A_i denotes an aggregate characterized by its mass i, or equivalently, a group characterized only by the number of its component individuals. Recently, many researches have been carried out to study the migration-driven (or equivalently, exchange-driven) growth mechanism which frequently arises in physics and in social science [10–13]. Ispolatov and co-workers have introduced several kinetic exchange models to describe the wealth redistribution of individuals in economical activities [14]. Leyvraz and Redner have proposed a migration-driven growth model and provided some qualitative predictions of the evolution of city population [15]. In these models, the aggregates evolve according to the irreversible biased migration mechanism, $A_k+A_l\rightarrow A_{k-1}+A_{l+1}$ $(k\leq l)$. That is, a larger aggregate of size l gains one monomer from a smaller aggregate of size k, while the reverse process is forbidden. The results have exhibited that the kinetics of the migration-driven aggregate growth falls in a different scaling regime as compared to those conventional binary coagulation processes. Generally, monomer migrations could go from the larger to the smaller aggregates as well as from the smaller to the larger. Ben-Naim and Krapivsky have studied a class of exchange-driven growth processes and their results can be applied to coarsening in the infinite range Ising-Kawasaki model and in the electrostatically driven granular layers [16]. In our previous works [17,18], we have investigated the kinetics of the migration-driven aggregation model with a size-dependent unbiased rate kernel and found that the aggregate size distribution approaches the conventional scaling form. Thus it is believed that such migration-driven aggregation processes, as well as those conventional binary coagulation processes, can give rise to rich evolution kinetics.

It should also be pointed out that most of those works on aggregate growth phenomena have been performed by means of the mean-field rate equation or by Monte Carlo simulation. In the mean-field framework, the system is assumed to be spatial homogeneity and the fluctuations in the densities of reactants is negligible. Thus the aggregates are considered to be homogeneously distributed in the space throughout the process and the reaction between any two aggregates is assumed to be completely random, while in Monte Carlo simulations [5,6], the aggregates are put onto lattice sites, and the coagulation reaction occurs whenever two aggregates occupy the same lattice site. Such an aggregate growth process can be regarded as a network, in which the nodes are the temporal "lodgements" of the aggregates and the links represent the reactions between two aggregates. Obviously, in theoretical works, an aggregate growth process is modeled as a completely random graph, while the simulations of aggregate growth are carried out on a regular network. Both theoretical and simulation investigations have been performed assuming that all nodes (i.e., aggregates) in the networks have approximately the same degree of "links," namely, the same number of contacts with other nodes. However, natural and social situations are rarely well described by such random or regular networks. Despite the different natures of their elements and interactions among the elements, the complex weblike

*Electronic address: kejianhong@yahoo.com.cn
†Electronic address: xschen@mail.sitp.ac.cn

structures of many distinct real-world systems have been found to have a common feature: their degree distributions take a scale-free power-law form [19]. Let $P(k)$ be the probability of a node with k links, and the power-law degree distribution can then be expressed as $P(k) \sim k^{-\gamma}$, where the exponent γ denotes the degree properties of scale-free networks (SFNs). In both natural and artificial networks, γ is usually in the range of $2 < \gamma < 3$ [20].

Since the topology of scale-free networks deviates from that of the homogeneous regular lattices and random graphs, the conventional models (such as Ising model, epidemic model, percolation model, and so on) on SFNs exhibit dynamic behaviors quite different from those obtained in traditional ways [21–24]. Moreover, Gallos and Argyrakis have found that the chemical reactions of the model systems of $A+A \rightarrow 0$ and $A+B \rightarrow 0$ performed on SFNs exhibit drastically different behaviors as compared to the same reactions in normal space [25]. Catanzaro *et al.* have presented a detailed analytical study of the $A+A \rightarrow 0$ diffusion-annihilation process in uncorrelated SFNs [26], and Gallos *et al.* have compared the same reaction-diffusion process on SFNs created with either the configuration model or the uncorrelated configuration model [27]. Laguna *et al.* have investigated the static annihilation on complex networks to obtain the temporal evolution of the distribution of surviving sites with an arbitrary number of connections [28]. These works have verified that the aggregate growth proceeding on SFNs can reveal intriguing evolution behaviors. To the best of our knowledge, such investigations combining kinetic migration processes and complex networks remain unexplored.

In this work, we investigate the kinetics of the migration-driven aggregate growth on completely connected scale-free networks. In the system, the aggregates evolve according to a nondirectional migration reaction,

$$A_{kl} + A_{ij} \xrightarrow{K(k;l|i;j)} A_{k-1,l} + A_{i+1,j},$$

where A_{kl} denotes an aggregate of size k occupying a node with l links and $K(k;l|i;j)$ denotes the rate at which one monomer is transferred from the aggregates A_{kl} to A_{ij}. This model interpolates between the migration-driven aggregate growth model on completely random graphs and that on regular lattices. We believe that the migration systems on SFNs are of interest in studying the scaling properties of their evolution behaviors. Employing the rate equation approach, we have determined the analytical solution of our model and found that in the long-time limit, the aggregate size distribution does approach a scaling form different from that of the corresponding migration system in homogenous space.

It is also believed that the model of migration-driven growth on SFNs can mimic many phenomena in natural and social science, such as the county population distribution. It has been argued that the growth of city population may be attributed, to a great extent, to population migrations [15]. And the population distribution $c_k(t)$ of large cities is found to obey the Zipf's law [29] and takes the power-law form, $c_k(t) \sim k^{-\theta}$. For many countries, the exponent θ is larger than 2 [11,30]. However, for conventional migration models [15,18], the exponent θ is always smaller than 2. In fact, the rate of population migrations between two cities has relation with their traffic status. And the unbalanced economic development of different cities may also play an important role in population migrations. Such realistic factors can be merged into the weight of the traffic between different cities. Thus it is more reasonable that realistic population migrations proceed on weighted traffic networks, in which the nodes are the sites of cities and the weighted link degrees are the number of traffic connections (such as railways and highways) between cities. Recent works have exhibited that the weighted traffic networks may have a scale-free topology [31]. The general homogeneous case of our model, with $K(k;l|i;j) \sim k^u i^v (lj)^\nu$, has been investigated in Ref. [32]. The results have exhibited that the exponent θ can indeed be larger than 2 if the indexes of the rate kernel satisfy a certain inequality. Moreover, the analytical results are in good agreement with the data of the population distribution of all U.S. counties. In this work, we shall further investigate and extend the previous work presented in Ref. [32].

The rest of the paper is organized as follows. In Sec. II, we propose a migration-driven aggregate growth model with a size and link dependent product kernel, and investigate the rate equation to obtain the aggregate size distribution. In Sec. III, we discuss the kinetic behavior of the model with a generalized kernel. In Sec. IV, we also give a simplified migration-driven growth model and then discuss the evolution behavior of the system. In Sec. V, we use our analytical results to imitate the data of the population distributions of all U.S. counties during the past century. A brief summary is given in Sec. VI.

II. ANALYTICAL SOLUTION OF THE MODEL WITH A PRODUCT RATE KERNEL

In this section, we investigate the kinetics of the migration-driven growth on scale-free networks by means of the rate equation approach. It is considered that the monomer migration reaction proceeds at a rate proportional to the concentrations of reactants. At time t, the concentration of the k-mer aggregates which occupy the nodes with l links connected to other nodes is set to be $a_{kl}(t)$. Then the rate equation for our system reads [32]

$$\frac{da_{kl}}{dt} = a_{k+1,l} \sum_{i,j} K(k+1;l|i;j) a_{ij} + a_{k-1,l} \sum_{i,j} K(i;j|k-1;l) a_{ij} - a_{kl} \sum_{i,j} [K(k;l|i;j) + K(i;j|k;l)] a_{ij}. \quad (1)$$

As our motivation is to investigate analytically the dependence of the aggregate growth kinetics on the topology of scale-free networks, we assume that the rate kernel $K(k;l|i;j)$ is dependent on the number of the links connected to the immigrant or emigrant aggregates, $K(k;l|i;j) \sim l^\nu j^\nu$. When $\nu=0$, our model reduces to the well-understood random migration case [16–18]. For most practical situations, $\nu > 0$. Moreover, the rate, at which one monomer migrates from the aggregates A_{kl} to A_{ij}, is proportional to the values k^u and i^v, at least for large k and i. Here, u and v are constant

indexes which can interpret the degree of "richness" in the population of a city (or equivalently, a county). When the values of u and v increase, the aggregate becomes much generous in emigration and much greedy in immigration. In the context of city population growth, it is sound that the city with large population and convenient traffic has more susceptible emigrants and also attracts more potential immigrants than the traffic-inconvenient small city [32]. The restriction of the rate kernel follows the spirit in which the conventional migration-driven growth model is formulated [15,16]. Further, we consider a simplest but important case in which there only exist the monomer aggregates at $t=0$ and their concentration is equal to unity. And the degree distribution of the nodes occupied by initial monomers takes the scale-free power-law form, $P(l)\sim l^{-\gamma}$ $(\gamma>2)$. The monodisperse initial condition is then given as follows:

$$a_{kl}(0)=(\gamma-1)l^{-\gamma}\delta_{k1}, \tag{2}$$

where the term $\gamma-1$ is the normalization factor, and the rate kernel takes the form

$$K(k;l|i;j)=Kk^{u}i^{v}(lj)^{v}, \tag{3}$$

where K is a constant. Without any loss of generality, we can set the coefficient $K=1$. Practically, the link number l of a node must be no larger than the cutoff value l_{max}. Further, it can also be concluded, by analyzing the structure of the rate equation (1), that the value range of the link number l has almost no effect on the concrete form of the solution $a_{kl}(t)$. For the convenience of algebra, we assume that the link number can vary from 1 to ∞. We then determine the analytical solution of Eq. (1) in two distinct systems as follows.

A. Symmetrical system

We first consider the case with the symmetrical rate kernel, i.e., $u=v=\mu$. Substituting Eq. (3) into the governing rate equation (1), we obtain

$$\frac{da_{kl}}{dt}=l^{\nu}[(k+1)^{\mu}a_{k+1,l}+(k-1)^{\mu}a_{k-1,l}-2k^{\mu}a_{kl}]\sum_{i,j}i^{\mu}j^{\nu}a_{ij}. \tag{4}$$

Introducing the new variable, $T(t,l)=\int_0^t dt' l^{\nu}\Sigma_{i,j}i^{\mu}j^{\nu}a_{ij}(t')$, we then recast Eq. (4) to the following discrete equation:

$$\frac{da_{kl}}{dT}=(k+1)^{\mu}a_{k+1,l}+(k-1)^{\mu}a_{k-1,l}-2k^{\mu}a_{kl}. \tag{5}$$

Equation (5) is similar to the governing rate equation for the conventional migration-driven growth model with the symmetrical rate kernel $K(i;j)\sim(ij)^{\mu}$ [16,18]. Employing the technique introduced in Ref. [18], one can then deduce the analytical solution $a_{kl}(T)$ of Eq. (5).

Under the above monodisperse initial condition, we can make a scaling ansatz that the solution $a_{kl}(T)$ $(k\geq 1)$ of Eq. (5) can take the uniform scaling form [7]

$$a_{kl}(T)=l^{-\lambda}k^{-\tau}T^{-\tilde{w}}\Phi[k/S(T,l)], \quad S(T,l)\propto T^{\tilde{z}}. \tag{6}$$

Here, $S(T,l)$ denotes the typical size of the aggregates locating on the nodes with l links, which plays a role analogous to that of the correlation length in critical phenomena. Moreover, the scaling function $\Phi(x)\simeq 1$ for $x\ll 1$ and $\Phi(x)\simeq 0$ for $x\gg 1$ [7]. The scaling form (6) also implies that $T(t,l)$ should grow infinitely with time t. Multiplying Eq. (5) with k and summing them up over all k and l, we obtain $\dot{M}_1(T)=\Sigma_{k,l}k\dot{a}_{kl}(T)=0$. So, our model obeys the mass conservation law. One can then deduce that the scaling exponents of the form (6) have the relation $\tilde{w}=(2-\tau)\tilde{z}$. Moreover, since the only physically meaningful values of $\tilde{w}$ and $\tilde{z}$ are both larger than zero, τ must be less than 2 [7]. Thus Eq. (6) can be rewritten as

$$a_{kl}(T)=l^{-\lambda}k^{-\tau}[S(T,l)]^{\tau-2}\Phi[k/S(T,l)], \quad S(T,l)\propto T^{\tilde{z}}. \tag{7}$$

Then the problem is reduced to determining the scaling function $\Phi(x)$, the typical size $S(T,l)$, and the scaling exponents (λ and τ).

We first determine the typical size $S(T,l)$ and those scaling exponents. By summing up Eq. (5) we readily obtain

$$\frac{dM_{l0}}{dT}=-a_{1l}, \quad \frac{dM_{l2}}{dT}=2M_{l\mu}, \tag{8}$$

with the shorthand notation $M_{l\mu}(T)=\Sigma_{k=1}^{\infty}k^{\mu}a_{kl}(T)$. Substituting Eq. (7) into Eq. (8), we deduce two sets of evolution equations for the typical size $S(T,l)$ in several different cases (such as the $\tau>\mu+1$, $\tau=\mu+1$ and $\tau<\mu+1$ cases). The details of this derivation are similar to those given in Ref. [18]. Making a detailed comparison between these resulting equations, one can then deduce $\tau=\mu-1$ and

$$\frac{dS(T,l)}{dT}\sim[S(T,l)]^{\mu-1}. \tag{9}$$

Equation (9) can be straightforwardly solved to yield the asymptotical solution for $\mu<2$,

$$S(T,l)\propto[(2-\mu)T]^{1/(2-\mu)}. \tag{10}$$

On the other hand, providing that the scaling ansatz (6) is also valid for $\mu>2$, from Eq. (9) we will deduce the self-contradictory solution $S(T,l)\propto[(\mu-2)(T_c-T)]^{1/(2-\mu)}$, where T_c is a finite positive quantity. So, the system may evolve according to a scheme different from the above scaling form in the $\mu>2$ case. It is found that for the corresponding migration system in normal space, an instantaneous and complete gelation may take place for $\mu>2$ [16]. As for the special case of $\mu=2$, the aggregate size distribution can take the exponential-correction scaling form, $a_{kl}(T)=l^{-\lambda}k^{-\tau}[S(T,l)]^{\tau-2}\Phi[k/S(T,l)]$, with $S(T,l)\propto(e^T)^{\tilde{z}}$. In this work, we focus only on the solvable case of $\mu<2$, in which the solution of Eq. (5) consistently takes the scaling form (6) and can be analytically obtained.

Then we further determine the t-dependent expression of the typical size $S(t,l)$ in the $\mu<2$ case. According to the definition of $T(t,l)$, we obtain

$$\frac{dT}{dt} = l^{\nu} \sum_{i,j} i^{\mu} j^{\nu} a_{ij}(T). \tag{11}$$

Substituting the scaling ansatz (7) into Eq. (11), we can readily determine the analytical solution of $T(t,l)$ and then obtain the expression of $S(t,l)$ as follows:

$$S(t,l) \sim \begin{cases} t^{1/(3-2\mu)} l^{\nu/(2-\mu)} & \text{if } \mu < 3/2, \\ \exp(C_1 t) l^{2\nu} & \text{if } \mu = 3/2, \\ (t_c - t)^{1/(3-2\mu)} l^{\nu/(2-\mu)} & \text{if } 2 > \mu > 3/2, \end{cases} \tag{12}$$

where C_1 is a positive integration constant and t_c denotes a finite critical time. It should be pointed out that the critical time t_c can be determined if all initial details of the reaction event are given. The results show that for the system with $2>\mu>3/2$, the typical size diverges at a finite critical time t_c and therefore a gelation transition may emerge at this time point (see, e.g., Refs. [8,33,34]). This phenomenon has also been observed in the conventional migration processes in normal space [16,18]. Moreover, it is worth noting that the solution (12) of the typical size $S(t,l)$ is valid only for $\lambda > 1+\nu/(2-\mu)$ if the link number l varies from 1 to infinity. In more realistic real-world systems, since the link number of a node has the cutoff value l_{max}, the indexes may no longer be called for the restriction $\lambda > 1+\nu/(2-\mu)$.

Next, by summing up Eq. (4) we obtain $\Sigma_{k=0}^{\infty} \dot{a}_{kl}(t)=0$, which yields $\Sigma_{k=0}^{\infty} a_{kl}(t) \equiv (\gamma-1) l^{-\gamma}$. Since $M_{l0}(t) \to 0$ at $t \to \infty$, we can deduce $a_{0l}(t) \sim l^{-\gamma}$ at large times. Substituting the scaling ansatz (6) into Eq. (5), we find $\lambda = \gamma - \nu/(2-\mu)$.

Finally, we determine the scaling function $\Phi(x)$. The scaling ansatz (7) can be supposed to be valid for all nongelling systems and also for the gelling cases near the vicinity of the gelation point t_c [8]. Inserting Eq. (7) into Eq. (5), we obtain the differential equation of the scaling function $\Phi(x)$ as follows:

$$x\Phi''(x) + (2 + px^{2-\mu})\Phi'(x) \simeq p(\mu-3)x^{1-\mu}\Phi(x), \tag{13}$$

where p is such a separation constant satisfying the relation $dS(T,l)/dT = p[S(T,l)]^{\mu-1}$. Equation (13) can be readily solved to yield

$$\Phi(x) \simeq C_3 \exp(-C_2 x^{2-\mu}), \tag{14}$$

where $C_2 = p/(2-\mu)$ and C_3 is an integration constant. Since our system obeys the mass conservation law, C_3 and p are related as $\int_0^{\infty} dx C_3 x^{2-\mu} \exp(-C_4 x^{2-\mu}) \Sigma_l l^{-\lambda} = 1$. One can choose a suitable value for p in order to have $C_3 = 1$.

Thus we obtain the explicit analytical solution of the aggregate size distribution $a_{kl}(t)$. For the nongelling system with $\mu < 3/2$, $a_{kl}(t)$ consistently takes the following scaling form at large times:

$$a_{kl}(t) \simeq C_5 l^{-\gamma-\nu} k^{1-\mu} t^{-(3-\mu)/(3-2\mu)} \exp(-C_2 x^{2-\mu}), \quad x = C_4 k t^{-1/(3-2\mu)} l^{-\nu/(2-\mu)}, \tag{15}$$

where $C_5 = C_4^{\mu-3}$ and C_4 is a positive constant. Letting $\nu^* = \nu(3-2\mu)/(2-\mu)$ and $\gamma^* = \gamma + \nu(\mu-1)/(2-\mu)$ and then omitting the superscripts, one can rewrite Eq. (15) as the corresponding expression of the aggregate size distribution given in Ref. [32],

$$a_{kl}(t) \sim l^{\mu\nu/(3-2\mu)-\gamma} k^{-2} x^{3-\mu} \exp(-C_2 x^{2-\mu}), \quad x \simeq k(tl^{\nu})^{-1/(3-2\mu)}. \tag{16}$$

Such substitutions are done for the sake of consistency in the expression of the typical size with the following asymmetrical system. Obviously, for a given l, Eq. (15) can reduce to the conventional scaling form

$$a_{kl}(t) \sim k^{-\tau} t^{-w} \Phi[k/S(t)], \quad S(t) \propto t^{z}, \tag{17}$$

where the exponents have the relation $w=(2-\tau)z$. For this case, $\tau = \mu - 1$ and $z = 1/(3-2\mu)$.

For the special case of $\mu = 3/2$, the aggregate size distribution approaches the exponential-correction scaling form

$$a_{kl}(t) \sim l^{-\gamma-\nu} k^{-1/2} e^{-C_6 t} \exp(-C_2 x^{1/2}), \quad x \simeq k \exp(-C_1 t) l^{-2\nu}, \tag{18}$$

where $C_6 = 3C_1/2$. While for the gelling system with the index $2>\mu>3/2$, the pre-gelation solution of the aggregate size distribution $a_{kl}(t)$ $(t \to t_c)$ also takes the scaling form

$$a_{kl}(t) \sim l^{-\gamma-\nu} k^{1-\mu} (t_c - t)^{-(3-\mu)/(3-2\mu)} \exp(-C_2 x^{2-\mu}), \quad x \simeq k(t_c - t)^{-1/(3-2\mu)} l^{-\nu/(2-\mu)}. \tag{19}$$

Obviously, for the $2>\mu>3/2$ case, each $a_{kl}(t)$ decays with time and vanishes at the gelation point t_c. Thus an infinite aggregate containing all the mass of the system forms at the critical time t_c and $a_{kl}(t)=0$ for $t \geq t_c$, namely, the gelation is complete. It is surprisingly different from conventional aggregation processes [8,33], in which the gel aggregate contains only a certain percent of the entire mass of the system at the gelation point t_c and the gel aggregate then continuously grows by merging the remaining finite aggregates after the gelation transition. Such a phenomenon has also been studied in detail in Ref. [16].

It is also of great interest to determine the total distribution $c_k(t)$ of all the aggregates with the same size k, $c_k(t) = \Sigma_{l=1}^{\infty} a_{kl}(t)$, which is the corresponding aggregate size distribution $a_k(t)$ in conventional migration-driven growth models (see, e.g., Refs. [16–18]). Here we pay more attention to the more interesting nongelling case of $\mu < 3/2$, in which the system infinitely evolves in time according to the scaling regime. By using Eq. (15) we obtain

$$c_k(t) \simeq k^{-\xi} t^{-\zeta} \Psi(y), \quad y = C_4 k t^{-1/(3-2\mu)}, \tag{20}$$

where $\xi = 1 + (\gamma-1)(2-\mu)/\nu$, $\zeta = [1-(\gamma-1)(2-\mu)/\nu]/(3-2\mu)$, and the scaling function

$$\Psi(y) = C_7 \int_0^{C_2 y^{2-\mu}} Z^{(\gamma-1)/\nu} \exp(-Z) dZ, \tag{21}$$

where $C_7 = C_5 \nu^{-1} (C_2 C_4^{2-\mu})^{-(\gamma+\nu-1)/\nu}$. From Eq. (20) we deduce that for $1 \ll k \ll t^{1/(3-2\mu)}$, $c_k(t)$ takes the power-law form as follows [32]:

$$c_k(t) \sim k^{1-\mu} t^{-(3-\mu)/(3-2\mu)}, \tag{22}$$

while for $k \gg t^{1/(3-2\mu)}$, it takes another power-law form [32],

$$c_k(t) \sim k^{-\xi} t^{-\zeta}. \tag{23}$$

In the ordinary migration-driven aggregate growth system with the same rate kernel, it has exhibited that the aggregate size distribution approaches the consistent scaling form $c_k(t) \sim k^{1-\mu} t^{-(3-\mu)/(3-2\mu)} \exp(-C_2 y^{2-\mu})$, with the scaling variable $y \propto k t^{-1/(3-2\mu)}$ [18]. Obviously, the size distribution of the aggregates with size $1 \ll k \ll t^{1/(3-2\mu)}$ in this system is identical with that in ordinary migration models. But, for the large aggregates with size $k \gg t^{1/(3-2\mu)}$, the size distribution in this system decays as a power law, while in conventional systems it decays exponentially [18]. Thus the kinetic evolution of the migration-driven aggregate growth on completely connected scale-free networks is quite different from that in normal space. The most interesting result of this model is that, when the indexes satisfy the inequality $\nu < (\gamma-1)(2-\mu)$, the size distribution of the large aggregates with size $k \gg t^{1/(3-2\mu)}$ unexpectedly increases with time. Moreover, for a given time, the total size distribution of large aggregates evolves as a power law in size k, $c_k(t) \sim k^{-\xi}$.

B. Asymmetrical system

Next, we investigate the general case with the asymmetrical rate kernel (3), i.e., $u \neq v$, which can further verify the above intriguing behavior of the total size distribution. The governing rate equation (1) can be reduced to

$$\frac{da_{kl}}{dT} = [(k+1)^u a_{k+1,l} - k^u a_{kl}] \sum_{i,j} i^v j^\nu a_{ij} + [(k-1)^v a_{k-1,l} - k^v a_{kl}] \sum_{i,j} i^u j^\nu a_{ij}, \tag{24}$$

with the variable $T(t,l) = t l^\nu$. Following a spirit similar to the above symmetrical case, we also make the above-mentioned scaling ansatz (7) for the aggregate size distribution in this asymmetrical system.

Summing up Eq. (24) over all k yields

$$\frac{dM_{l0}}{dT} = -a_{1l} W_{v\nu}, \quad \frac{dM_{l2}}{dT} = (M_{lu} - 2M_{l,u+1}) W_{v\nu} + (M_{lv} + 2M_{l,v+1}) W_{u\nu}, \tag{25}$$

with the shorthand notation $W_{u\nu}(T) = \sum_{i,j=1}^{\infty} i^u j^\nu a_{ij}(T)$. Substituting the scaling ansatz (7) into Eq. (25), one can obtain two sets of evolution equations for the typical size $S(T,l)$. A detailed comparison between these resulting equations shows that the scaling ansatz is valid only under the condition of $u < v$ and $u < 1$. If $u > v$, we find $dS(T,l)/dT < 0$ in the long-time limit and the scaling ansatz (7) is thus invalid. So, for the $u > v$ case, infinite aggregates cannot be formed and only monomer aggregates can survive finally, which is identical with the corresponding result found in Ref. [18]. As for the system with $u < v$ and $u > 1$, a gelation transition may take place at a finite critical time.

In this asymmetrical case, we also focus only on the kinetic scaling behavior of the nongelling system with $u < v$ and $u < 1$. In the nongelling case, we deduce, by using the scaling ansatz (7), that $\tau = u$ and

$$\frac{dS(T,l)}{dT} \sim [S(T,l)]^{u+v-1}. \tag{26}$$

Since $T(t,l) = t l^\nu$, we solve Eq. (26) and then obtain the t-dependent solution of the typical size,

$$S(t,l) \propto [(2-u-v) t l^\nu]^{1/(2-u-v)}, \tag{27}$$

which is valid only for $u+v < 2$. For the case with $u+v > 2$, the scaling ansatz of the aggregate size distribution is invalid and the system will undergo a gelation transition after a certain finite time. As for the borderline case of $u+v=2$, the aggregate size distribution can take the exponential-correction scaling form of Eq. (7), with the typical size $S(T,l)$ increasing exponentially with time. On the other hand, for this asymmetrical system, we also have $\sum_{k=0}^{\infty} \dot{a}_{kl}(t) = 0$. By employing a technique similar to that used in the above symmetrical system, one can readily find $\lambda = \gamma - \nu v/(2-u-v)$.

We then determine the scaling function $\Phi(x)$ in the nongelling system with $u+v < 2$ and $u < 1$. We find, by substituting Eq. (7) into Eq. (24), that the scaling function satisfies the following differential equation:

$$(C_8 x^v - C_9 x^u - q x) \Phi'(x) \simeq [q(2-u) - C_8 (v-u) x^{v-1}] \Phi(x), \tag{28}$$

where $C_8 = \Sigma_l l^{\nu-\lambda} \int_0^\infty dx \Phi(x)$, $C_9 = \Sigma_l l^{\nu-\lambda} \int_0^\infty dx [x^{v-u} \Phi(x)]$, and q is a constant satisfying the equation $dS(T,l)/dT = q[S(T,l)]^{u+v-1}$. It is difficult to derive the consistent analytical solution of $\Phi(x)$ from Eq. (28). For small x, we obtain the asymptotical solution

$$\Phi(x) \simeq C_{12} \exp(-C_{10} x^{1-u} + C_{11} x^{v-u}), \tag{29}$$

where $C_{10} = q(2-u)/[(1-u)C_9]$, $C_{11} = C_8/C_9$, and C_{12} is an integration constant. For $x \gg 1$,

$$\Phi(x) \simeq \begin{cases} x^{-(v-u)} & \text{if } v > 1, \\ x^{-\kappa} & \text{if } v = 1, \\ x^{-(2-u)} & \text{if } v < 1, \end{cases} \tag{30}$$

where $\kappa = 1 - u + q/(q - C_8)$ $(q \neq C_8)$. Moreover, it follows from Eq. (28) that the scaling function $\Phi(x)$ has singularity at the point x_c (here, x_c satisfies the equation $C_8 x_c^v - C_9 x_c^u - q x_c = 0$). Under the monodisperse initial condition, the scaling function $\Phi(x)$ may be discontinuous and $\Phi(x) = 0$ for all $x > x_c$. This is in agreement with the argument of discontinuity of the scaling function in Ref. [15].

Thus in the nongelling system with $u+v < 2$ and $u < 1$, the size distribution $a_{kl}(t)$ of the aggregates with size $1 \ll k \ll C_{13} (t l^\nu)^{1/(2-u-v)}$ approaches the following scaling form:

$$a_{kl}(t) \sim l^{-\gamma-\nu} k^{-u} t^{-(2-u)/(2-u-v)} \exp(-C_{10} x^{1-u} + C_{11} x^{v-u}), \qquad x = C_{13}^{-1} k (t l^\nu)^{-1/(2-u-v)}, \tag{31}$$

where $C_{13} = [q(2-u-v)]^{1/(2-u-v)}$. For $k \gg C_{13} (t l^\nu)^{1/(2-u-v)}$, $a_{kl}(t) \simeq 0$.

Finally, we determine the total size distribution $c_k(t)$ of all the aggregates with the same size k. For $1 \ll k \ll t^{1/(2-u-v)}$, $c_k(t)$ takes the power-law form [32]

$$c_k(t) \sim k^{-u} t^{-(2-u)/(2-u-v)}, \tag{32}$$

which is similar to that in the ordinary migration-driven growth model with the same rate kernel [18]. For $k \gg t^{1/(2-u-v)}$, $c_k(t)$ approaches another power-law form [32],

$$c_k(t) \sim k^{-\alpha} t^{-\beta}, \tag{33}$$

where $\alpha = 2 - v + (\gamma - 1)(2-u-v)/\nu$ and $\beta = v/(2-u-v) - (\gamma - 1)/\nu$. Equation (33) shows that the total size distribution of the aggregates with size $k \gg t^{1/(2-u-v)}$ in our model is drastically different from that of the same system in normal space [18]. Similar to the above symmetrical system, the size distribution of the large aggregates with size $k \gg t^{1/(2-u-v)}$ in this asymmetrical case can also singularly increase with time, if the indexes satisfy the inequality $v\nu < (2-u-v)(\gamma-1)$. Moreover, for a given time, the total size distribution of large aggregates also decays as a power law in size, $c_k(t) \sim k^{-\alpha}$.

III. MODEL WITH A GENERALIZED RATE KERNEL

In order to thoroughly understand the kinetics of the migration-driven aggregate growth on SFNs, we also investigate the model with the generalized symmetrical kernel $K(k;l|i;j) = (k^v i^\omega + k^\omega i^v)(lj)^\nu$. The kernel is a typically homogeneous function of the reactants' sizes k and i. Obviously, if $v = \omega$, this generalized model will reduce to the model with the symmetrical product kernel in Sec. II. Since the kernel is symmetrical, we can set $\omega > v$ without losing any generality. Introducing the scaling time $T(t,l) = tl^\nu$, we then rewrite Eq. (1) as follows:

$$\frac{da_{kl}}{dT} = W_{v\nu}[(k+1)^\omega a_{k+1,l} + (k-1)^\omega a_{k-1,l} - 2k^\omega a_{kl}] + W_{\omega\nu}[(k+1)^v a_{k+1,l} + (k-1)^v a_{k-1,l} - 2k^v a_{kl}], \tag{34}$$

which is similar to the governing rate equation for an exchange-driven growth model in Ref. [16]. Equation (34) can be analytically solved by employing the technique introduced in Sec. II.

We assume that the scaling ansatz (6) still hold in the system with the generalized rate kernel. By summing up Eq. (34) one can obtain

$$\frac{dM_{l2}}{dT} = 2(M_{l\omega}W_{v\nu} + M_{lv}W_{\omega\nu}), \quad \frac{dM_{l0}}{dT} = -a_{1l}(W_{v\nu} + W_{\omega\nu}). \tag{35}$$

Substituting Eq. (7) into Eq. (35), we deduce two sets of evolution equations of the typical size $S(T,l)$ and then make a detailed comparison between these resulting equations. It is found that the modified scaling ansatz (7) is valid only in the system with $v + \omega < 3$, while for the $v + \omega > 3$ case, the scaling form (7) is invalid and a gelation transition arises.

For this model, we also investigate only the kinetic scaling behavior of the nongelling system with $v + \omega < 3$. From Eq. (35) we deduce that the scaling exponent $\tau = v - 1$ and the asymptotical behavior of $S(T,l)$ is

$$\frac{dS}{dT} \sim S^{v+\omega-2}. \tag{36}$$

By solving Eq. (36) and inserting $T(t,l) = tl^\nu$ we deduce the asymptotical solution of $S(t,l)$ in the $v + \omega < 3$ case,

$$S(t,l) \propto [(3 - v - \omega)tl^\nu]^{1/(3-v-\omega)}. \tag{37}$$

On the other hand, making use of the method introduced in Sec. II, we deduce the exponent $\lambda = \gamma - \nu\omega/(3 - v - \omega)$ for this case.

Now, we determine the scaling function $\Phi(x)$ for the nongelling system. Substituting the scaling ansatz (7) into Eq. (34), we find the following differential equation:

$$(C_{14}x^{1+\omega-v} + C_{15}x)\Phi''(x) + [rx^{2-v} + 2C_{15} + 2C_{14}(1 + \omega - v)x^{\omega-v}]\Phi'(x) \simeq [r(v-3)x^{1-v} - C_{14}(1 + \omega - v)(\omega - v)x^{\omega-v-1}]\Phi(x), \tag{38}$$

where $C_{14} = \Sigma_l l^{\nu-\lambda} \int_0^\infty dx[x\Phi(x)]$, $C_{15} = \Sigma_l l^{\nu-\lambda} \int_0^\infty dx \times [x^{1+\omega-v}\Phi(x)]$, and r is a separation constant satisfying the equation $dS(T,l)/dT = r[S(T,l)]^{v+\omega-2}$. Since we have $v < \omega$, from Eq. (38) we can determine the asymptotical solution of the scaling function $\Phi(x)$ for $x \ll 1$,

$$\Phi(x) \simeq \begin{cases} \exp(-C_{16}x^{2-v}) & \text{if } \omega \geq 2, \\ \exp[-(C_{14}/C_{15})x^{\omega-v}] & \text{if } \omega < 2, \end{cases} \tag{39}$$

where $C_{16} = r/[(2-v)C_{15}]$ for $\omega > 2$ and $C_{16} = [r + C_{14}(2 - v)]/(2-v)C_{15}$ for $\omega = 2$. On the other hand, from Eq. (38) one can derive the following asymptotical solution for $x \gg 1$:

$$\Phi(x) \simeq \begin{cases} x^{-(\omega-v)} & \text{if } \omega > 2, \\ x^{-\varsigma} & \text{if } \omega = 2, \\ x^{2+\omega-v}\exp(-C_{17}x^{2-\omega}) & \text{if } \omega < 2, \end{cases} \tag{40}$$

where $C_{17} = r/[(2-\omega)C_{14}]$, $\varsigma = 3 - v$ for $r \geq C_{14}$, and $\varsigma = 2 - v + r/C_{14}$ for $r < C_{14}$. Equations (39) and (40) accord with the above restrictions on the scaling function $\Phi(x)$. However, it follows from Eq. (40) that C_{15} diverges for $\omega \geq 2$. Thus for the $\omega \geq 2$ case, $\Phi(x)$ must be discontinuous and can be consistently set to zero for all x greater than the critical value x_c in the system with the initial aggregates of any size having finite concentration; otherwise, a complete and instantaneous gelation transition may arise in an infinite initial system, as pointed out by Ref. [16].

Thus for the system with the generalized rate kernel, the aggregate size distribution $a_{kl}(t)$ strictly satisfies the scaling law in the case of $v < \omega < 2$ and $v + \omega < 3$,

$$a_{kl}(t) \sim l^{-\gamma-\nu}k^{1-\nu}t^{-(3-\upsilon)/(3-\nu-\omega)}\Phi(x), \quad x \simeq k(tl^{\nu})^{-1/(3-\nu-\omega)}, \tag{41}$$

where the scaling function $\Phi(x) \simeq \exp[-(C_{14}/C_{15})x^{\omega-\nu}]$ for small x and $\Phi(x) \simeq x^{2+\omega-\nu}\exp(-C_{17}x^{2-\omega})$ for large x. In other cases, the system may undergo a gelation transition after a certain finite time. The results show that for this generalized model, the kinetic behavior of aggregate growth is also crucially dependent on the reaction details such as the indexes of the rate kernel and the initial concentrations.

Finally, we determine the total size distribution $c_k(t)$ for this model. For $1 \ll k \ll t^{1/(3-\nu-\omega)}$,

$$c_k(t) \sim k^{1-\nu}t^{-(3-\upsilon)/(3-\nu-\omega)}, \tag{42}$$

which is similar to the corresponding conventional migration system in normal space [16]. While for $k \gg t^{1/(3-\nu-\omega)}$,

$$c_k(t) \sim k^{-\delta}t^{-\epsilon}, \tag{43}$$

where $\delta=2-\omega+(\gamma-1)(3-\nu-\omega)/\nu$ and $\epsilon=\omega/(3-\nu-\omega)-(\gamma-1)/\nu$. Similarly, we again observe that for the system with the generalized rate kernel, the size distribution of the large aggregates with size $k \gg t^{1/(3-\nu-\omega)}$ grows unexpectedly with time when $\omega\nu<(3-\nu-\omega)(\gamma-1)$.

IV. A SIMPLIFIED MIGRATION-DRIVEN GROWTH MODEL

In this section, motivated by the work of Marsili and Zhang [11], we propose a simplified but interesting model. In this system, the aggregate A_{kl} can spontaneously release monomers to let them walk randomly on scale-free networks with the possibility $I_1(k;l)$; meanwhile, the aggregate can also capture one of the randomly walking monomers with the possibility $I_2(k;l)$ when they pass by the node the aggregate locates. We assume that both the monomer gain and loss possibilities of the aggregate A_{kl} depend on its size k as well as the link degree l of the node it locates. Then the rate equation for this model reads

$$\frac{da_{kl}}{dt} = I_1(k-1;l)a_{k-1,l} + I_2(k+1;l)a_{k+1,l} - 2[I_1(k;l) + I_2(k;l)]a_{kl}. \tag{44}$$

We consider here a simple system in which the total mass is conserved. Moreover, we assume that both the monomer gain and loss possibilities of aggregates are monotonous functions of the aggregate size and the link degree (at least for large size and link degree). Thus we have $I_1(k;l)=I_2(k;l)$. For simplicity, we set $I_1(k;l)=I_2(k;l)=k^{\omega}l^{\nu}$. We again introduce the variable $T(t,l)=tl^{\nu}$ and then recast Eq. (44) to

$$\frac{da_{kl}}{dT} = (k-1)^{\omega}a_{k-1,l} + (k+1)^{\omega}a_{k+1,l} - 2k^{\omega}a_{kl}, \tag{45}$$

which is similar to the above differential equation (5). Thus we can readily deduce the scaling solution of Eq. (45) in the nongelling case of $\omega<2$,

$$a_{kl}(t) \simeq l^{\nu/(2-\omega)-\gamma}k^{-2}x^{3-\omega}\exp(-C_{18}x^{2-\omega}), \quad x = k(tl^{\nu})^{-1/(2-\omega)}, \tag{46}$$

where C_{18} is an integration constant. For the $\omega=2$ case, the aggregate size distribution takes the exponential-correction scaling form $a_{kl}(t) \simeq l^{-\gamma}k^{-2}x^{1-g}$, with $x=k\exp(-tl^{\nu})$ (here $g>1$). As for the $\omega>2$ case, a gelation transition will emerge at a finite critical time.

Further, we compute the total size distribution $c_k(t)$ in the $\omega<2$ case. For $1 \ll k \ll t^{1/(2-\omega)}$,

$$c_k(t) \sim k^{1-\omega}t^{(\omega-3)/(2-\omega)}. \tag{47}$$

For $k \gg t^{1/(2-\omega)}$,

$$c_k(t) \sim k^{-\phi}t^{-\psi}, \tag{48}$$

where $\phi=1+(\gamma-1)(2-\omega)/\nu$ and $\psi=1/(2-\omega)-(\gamma-1)/\nu$. Similar to the above-discussed models, the total size distribution of large aggregates can also grow unexpectedly if the indexes satisfy the inequality $\nu<(\gamma-1)(2-\omega)$.

V. APPLICATION TO THE DISTRIBUTION OF COUNTY POPULATION

The elementary migration mechanism underlies many fields of nature and social science. In this section, we apply our general theory of migration-driven growth on SFNs to the demography. Here, we test our predictions with the population distribution of all counties in the U.S. [35]. Practically, the demographic population growth also plays an important role in the evolution of county population. Following a spirit similar to Ref. [15], one can model the demographic population growth as the monomer birth process $A_{k,l} \to A_{k+1,l}$, with the rate kernel $J(k)$. The governing rate equation (1) is then rewritten as

$$\frac{da_{kl}}{dt} = a_{k+1,l}\sum_{i,j} K(k+1;l|i;j)a_{ij} + a_{k-1,l}\sum_{i,j} K(i;j|k-1;l)a_{ij} - a_{kl}\sum_{i,j}[K(k;l|i;j) + K(i;j|k;l)]a_{ij} + J(k-1)a_{k-1,l} - J(k)a_{kl}. \tag{49}$$

Figure 1 shows that during 1900–2000 the total population of the U.S. grows exponentially with time. Thus we can assume that the monomer birth kernel $J(k)=Jk$ (here J is a constant). In this realistic case, $J=0.0129\pm0.0003$.

For such a realistic case, we modify the scaling ansatz (6) as

$$a_{kl}(t) = e^{Jt}l^{-\lambda}k^{-\tau}[S(e^{Jt},l)]^{\tau-2}\Phi[k/S(e^{Jt},l)], \tag{50}$$

and have $M_1(t)=\Sigma_{k,l}a_{kl}(t) \sim e^{Jt}$ [32]. It is not difficult to verify, by substituting the modified scaling ansatz (50) into Eq. (49), that the scaling function and exponents of the scaling solution of Eq. (49) are the same as those of Eq. (1) in the case without demographic growth. Thus the distribution $a_{k,l}(t)/M_1(t)$ for the realistic system with population demographic growth is equivalent to the corresponding distribution $a_{k,l}(t)$ in Secs. II and III. Figure 2 exhibits that during

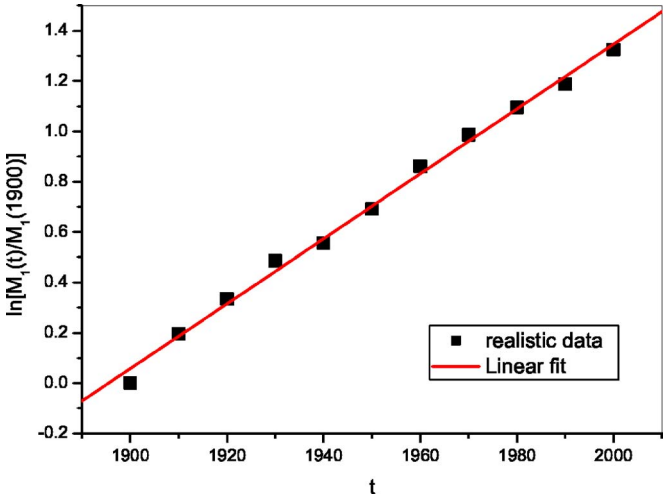

FIG. 1. (Color online) Semilog plot of the scaled total population $M_1(t)/M_1(1900)$ vs time t. The linear fit shows that the slope of the data line is 0.0129 ± 0.0003.

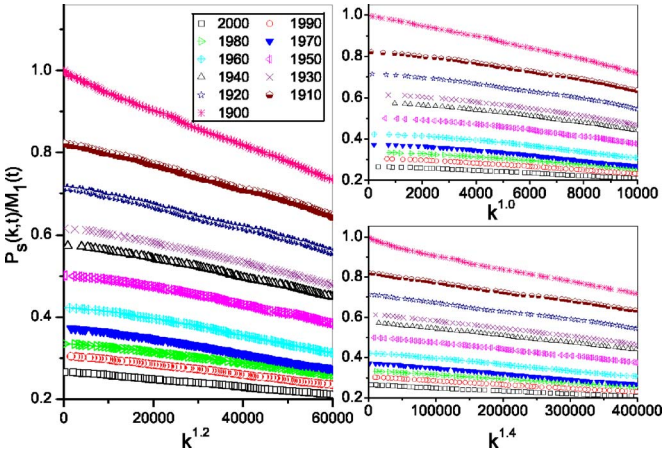

FIG. 3. (Color online) Plots of the cumulative size distribution $P_s(k,t)/M_1(t)$ vs different scaled size k. (i) Left plot: $P_s(k,t)/M_1(t)$ vs $k^{1.2}$. (ii) Upper-right plot: $P_s(k,t)/M_1(t)$ vs $k^{1.0}$. (iii) Lower-right plot: $P_s(k,t)/M_1(t)$ vs $k^{1.4}$. Here, $k\leq 10\,000$. Thus $P_s(k,t)/M_1(t)$ decays linearly with k^{η} for small k, where $\eta=1.2\pm0.2$.

1900–2000 the cumulative distribution of the counties with small population decays with time; while that of the counties with large population increases with time. This is in qualitative agreement with the theoretical predictions of our model. Moreover, almost all the distributions for large k approximately obey Zipf's law, $c_k(t)\sim k^{-\theta}$, with the exponent θ in the range of 2–3. Most intriguingly, the exponent θ predicted by our model can indeed be larger than 2 if the indexes of the symmetrical product rate kernel satisfy the inequality $\nu<(\gamma-1)(2-\mu)$ or those of the asymmetrical kernel satisfy $v\nu<(\gamma-1)(2-u-v)$, while those corresponding migration

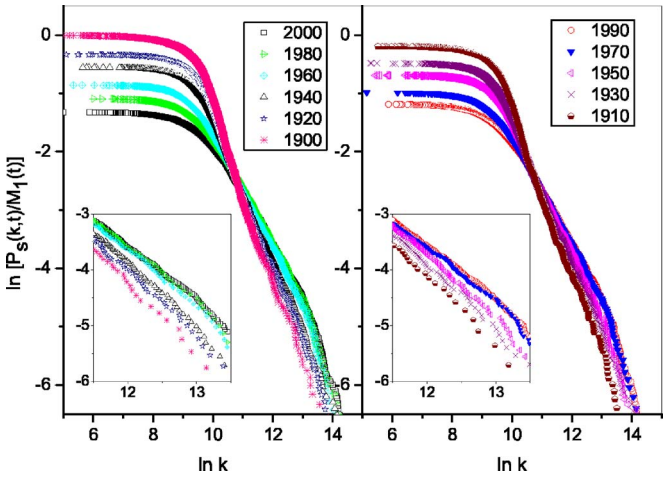

FIG. 2. (Color online) Log-log plots of the cumulative size distribution $P_s(k,t)/M_1(t)$ vs size k, where $P_s(k,t)=\Sigma_{j\geq k}c_j(t)$. Lower-left insets: the sections of the cumulative distributions in the range of $11.5\leq\ln k\leq 13.5$. The slopes of the data lines in the left inset are (i) 0.971 ± 0.002 for 2000; (ii) 1.010 ± 0.005 for 1980; (iii) 1.029 ± 0.005 for 1960; (iv) 1.172 ± 0.007 for 1940; (v) 1.160 ± 0.007 for 1920; (vi) 1.30 ± 0.02 for 1900 [32]. The slopes of the data lines in the right inset are (i) 0.982 ± 0.004 for 1990; (ii) 0.981 ± 0.005 for 1970; (iii) 1.135 ± 0.006 for 1950; (iv) 1.174 ± 0.008 for 1930; (v) 1.27 ± 0.01 for 1910.

models in normal space cannot do so [15–18]. Figure 2 also indicates that the slopes of the cumulative distributions of large-population counties vary for different years, while those of small-population counties asymptotically have the same value. Moreover, Fig. 3 further verifies that for small k, the cumulative size distribution $P_s(k,t)/M_1(t)\sim k^{\eta}$, with the exponent η almost independent of time. Thus there must exist more than one factor that may play important roles in the population evolution of the U.S. counties. It is well known that, besides the factor of the county's population size, some other factors, including the economic development and the traffic between counties, also play important parts in population migrations. And the economic development status of a county can be reflected, to a certain extent, in the traffic development of that county. Hence it is very much necessary to take the traffic connections (link degrees) between cities into account when we model the county population distribution [32]. Since the traffic networks in the U.S. always evolve continuously during 1900–2000, the indexes γ and ν introduced in the rate kernel may alter with time and therefore the exponent θ dependent on the indexes (γ and ν) may correspondingly vary for different decades as shown in Fig. 2.

We then use the analytical solution of the symmetrical migration system given in Sec. II to simulate the cumulative population distribution of all U.S. counties. In Eq. (22), the exponents of the power-law form depend only on the index μ that represents the factor of population size. We find, by analyzing the population data of the small U.S. counties, that $c_k(t)\sim k^{0.2\pm0.2}$ for small k (see Fig. 3). Thus in Eq. (15), $\mu=0.8\pm0.2$, and the exponents γ and ν have the relation $\xi=1.0+1.2(\gamma-1)/\nu$. The actual value of γ can be obtained by analyzing the weighted traffic networks of the U.S. In our previous work [32], we chose $\mu=0.8$ and $\gamma=2.1$ to fit the population distributions of all counties in the U.S. for every two decades during 1900–2000. The results have exhibited that the fitting curves are in good agreement with those realistic data. Moreover, we point out that the quantitative simu-

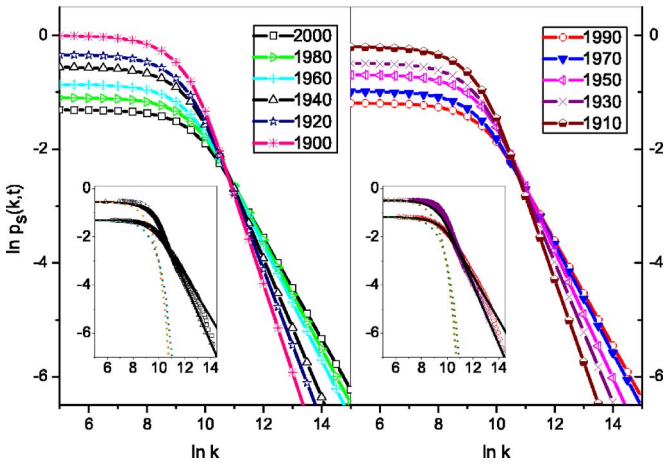

FIG. 4. (Color online) Log-log plots of the fitted cumulative size distribution $p_s(k,t)$ vs size k. Lower-left insets in both plots: log-log plot of the practical and fitted cumulative size distributions vs size k. In the left inset, the solid lines are our fitted size distributions for 2000 (lower) and 1940 (upper), while the curves with symbols (□ for 2000 and △ for 1940) are realistic population distributions (see, also, [32]). In the right inset, the solid lines are our fitted size distributions for 1990 (lower) and 1930 (upper), while the curves with symbols (∘ for 1990 and × for 1930) are realistic distributions. The dotted lines are the fitted distributions given by Ref. [16]. The comparisons between the realistic and fitted population distributions for the other years are similar to the above examples.

lations depend crucially on the value of ξ and the different choice of γ in the range of $2<\gamma<3$ can yield the similar results [32]. In order to verify this statement, we here use $\gamma=2.5$ as well as $\mu=0.8$ to fit the population data. Let $p_s(k,t)=C_{19}\int_k^\infty dx x^{0.2}\int_1^\infty dy y^{-2.5-1.8/(\xi-1.0)}\exp[-C_{20}x^{1.2}y^{-1.8/(\xi-1.0)}]$, the values of ξ, C_{19}, and C_{20} for different years can be well chosen by analyzing the corresponding population data. Figure 4 indicates that our simulation results are in quantitative agreement with the realistic population distributions almost for all k, except for very large k. The difference between the practical and fitted results in large k might be attributed to the fact that the actual limitation in the population size of a county has much more influence on the cumulative distribution of the counties with population number close to the cutoff value [32]. On the other hand, the simulation results given by the reversible migration model in normal space only cover the data for small k (see Fig. 4). So, the dependency of the rate kernel on link degrees causes a more crucial effect on $c_k(t)$ with large k than those with small k [see, e.g., Eqs. (22) and (23)]. It is also worth noting that the exponent μ asymptotically keeps the same quantity. Thus we can conclude that the topology of the traffic network in the U.S. does play a more important part in the population redistributions among counties during the 20th century. Moreover, it should be pointed out, by analyzing the structure of Eq. (1), that although the values of ν and γ in this realistic case may vary with time, $a_{kl}(t)$ can always take the same basic form for different years, except for the concrete values of those exponents and integration constants. Thus it is safe to say that our migration model on SFNs can provide useful qualitative predictions for the county (city) population distribution of a country. Further, if the traffic in a country has not developed so fast as to remarkably change the topology structure of the weighted traffic networks for a fairly long period, our migration model can also be used to quantitatively or semiquantitatively mimic the evolution behavior of the population distribution of that country.

On the other hand, the model with the asymmetrical product or generalized kernel can also be used to simulate the population size distribution of all counties in the U.S. if the values of the indexes of the rate kernels are correctly chosen based on the realistic data. Furthermore, providing that the simplified model proposed in Sec. IV is a reasonable candidate for this real-world case, Fig. 3 indicates that the index ω of the rate kernel must be 0.8 ± 0.2. Then Eq. (44) can be rewritten as

$$\frac{da_{kl}}{dt}=l^\nu[(k-1)^\omega a_{k-1,l}+(k+1)^\omega a_{k+1,l}-2k^\omega a_{kl}]+J(k-1)a_{k-1,l}-Jka_{kl}. \tag{51}$$

Obviously, when $\omega<1$, the last two terms in the right-side hand of Eq. (51) dominate over the first four terms, at least for large k. So, the scaling solution of Eq. (51) may be quite different from that of Eq. (44) in the case without demographic growth. This indicates that the simplified model is not suitable to interpret this realistic population distribution case for large k.

VI. SUMMARY

We have proposed an aggregate growth model on completely connected scale-free networks, in which the aggregates grow through the reversible monomer migrations between any two aggregates locating on different network nodes. By employing the rate equation approach, we have analyzed the evolution behavior of the size distribution of aggregates.

The system with the product kernel $K(k;l|i;j)\propto k^u i^v (lj)^\nu$ has been investigated. For the symmetrical system with $u=v=\mu$, the aggregate size distribution $a_{kl}(t)$ approaches the scaling form (6) in the $\mu<3/2$ case; while for the $\mu>3/2$ case, the system may undergo a complete gelation transition at a finite critical time. Additionally, the typical size $S(t,l)$ of the aggregates locating on the nodes with l links grows as $l^{\nu/(2-\mu)}t^{1/(3-2\mu)}$ in the nongelling case of $\mu<3/2$. For the asymmetrical system with $u\neq v$, $a_{kl}(t)$ approaches the scaling form (6) only in the case of $u+v<2$ and $u<1$. For the $u>v$ case, the typical aggregate size decays with time and therefore only monomer aggregates can survive finally. While for other cases, a gelation transition may take place in the system at a critical time point. In the nongelling case of $u+v<2$ and $u<1$, the typical size $S(t,l)$ grows as $(tl^\nu)^{1/(2-u-v)}$. Additionally, it is worth pointing out that for the asymmetrical system, the scaling exponent τ is dependent only on the index u for susceptible emigrations and independent of the index v for immigrations. Thus we can conclude that the susceptible monomer emigration of aggregates may play a more important role in the kinetics of the system than

the migrant acceptability of another aggregate [18]. Most intriguingly, for such migration-driven growth models on SFNs, the evolution behavior of the total size distribution $c_k(t)$ of the aggregates with the same size falls in two distinct regimes, which is quite different from the conventional migration systems in normal space.

For the system with the generalized symmetrical kernel $K(k;l|i;j) \propto (k^{\nu} i^{\omega} + k^{\omega} i^{\nu})(lj)^{\nu}$, the aggregate size distribution takes the scaling form (6) in the $\nu+\omega<3$ case, while the gelation transition can emerge after a sufficient long time in the $\nu+\omega>3$ case. It is also worth noting that an infinite initial system may undergo an instant and complete gelation transition in the case of $\max(\nu,\omega)>2$. In the nongelling case, the exponent τ of the scaling solution is always dependent only on the smaller one of the two indexes ν and ω, and the typical size $S(t,l)$ grows as $(tl^{\nu})^{1/(3-\nu-\omega)}$. Moreover, the total size distribution $c_k(t)$ also differs drastically from that in conventional migration systems in normal space.

The kinetic behavior of a simplified model has also been shown by considering the rate kernels $I_1(k;l)=I_2(k;l) \propto k^{\omega} l^{\nu}$. The aggregate size distribution takes the scaling form only in the $\omega<2$ case. While for the $\omega>2$ case, a gelation transition can arise in the system at a certain finite time. In the nongelling case, the typical size grows as $S(t,l) \propto (tl^{\nu})^{1/(2-\omega)}$. Similar to the above-discussed general migration models, the total size distribution $c_k(t)$ for large k is quite different from that for small k in this simplified model.

Finally, we have discussed the application of the migration-driven growth model on SFNs to the population distribution of counties in the U.S. Our results are in quantitative agreement with the realistic population data during 1900–2000. It is verified that our model can satisfactorily interpret the rule of the county population distribution.

ACKNOWLEDGMENTS

This project was supported by the National Natural Science Foundation of China (Grant No. 10305009 and Grant No. 60476040), by CNKBRSF (Grant No. 2001CB610407), and by the Natural Science Foundation of Zhejiang Province of China (Grant No. 102067).

[1] S. K. Friedlander, *Smoke, Dust and Haze: Fundamental of Aerosol Behavior* (Wiley, New York, 1977).
[2] J. Silk, *Star Formation* (Geneva Observatory, Sauverny, Switzerland, 1980).
[3] A. Pimpinelli and J. Villain, *Physics of Crystal Growth* (Cambridge University Press, Cambridge, U.K., 1998).
[4] P. Meakin, Rep. Prog. Phys. **55**, 157 (1992).
[5] R. M. Ziff, E. M. Hendriks, and M. H. Ernst, Phys. Rev. Lett. **49**, 593 (1982); P. Meakin, *ibid.* **51**, 1119 (1983); M. Kolb, R. Botet, and R. Jullien, *ibid.* **51**, 1123 (1983).
[6] K. Kang and S. Redner, Phys. Rev. A **30**, 2833 (1984).
[7] T. Vicsek and F. Family, Phys. Rev. Lett. **52**, 1669 (1984).
[8] P. G. J. van Dongen and M. H. Ernst, Phys. Rev. Lett. **54**, 1396 (1985).
[9] S. Song and D. Poland, Phys. Rev. A **46**, 5063 (1992).
[10] A. J. Bray, Adv. Phys. **43**, 357 (1994).
[11] D. H. Zanette and S. C. Manrubia, Phys. Rev. Lett. **79**, 523 (1997); M. Marsili and Y. C. Zhang, *ibid.* **80**, 2741 (1998).
[12] *The Theory of Income and Wealth Distribution*, edited by Y. S. Brenner *et al.* (St. Martin's Press, New York, 1988).
[13] L. A. N. Amaral, P. Gopikrishnan, V. Plerou, and H. E. Stanley, Physica A **299**, 127 (2001).
[14] S. Ispolatov, P. L. Krapivsky, and S. Redner, Eur. Phys. J. B **2**, 267 (1998).
[15] F. Leyvraz and S. Redner, Phys. Rev. Lett. **88**, 068301 (2002).
[16] E. Ben-Naim and P. L. Krapivsky, Phys. Rev. E **68**, 031104 (2003).
[17] J. Ke and Z. Lin, Phys. Rev. E **66**, 050102(R) (2002); Z. Lin and J. Ke, *ibid.* **67**, 031103 (2003).
[18] J. Ke, Z. Lin, and Y. Zhuang, Eur. Phys. J. B **36**, 423 (2003).
[19] R. Albert and A.-L. Barabási, Rev. Mod. Phys. **74**, 47 (2002); S. N. Dorogovtsev and J. F. F. Mendes, Adv. Phys. **51**, 1079 (2002).
[20] K. I. Goh, E. S. Oh, H. Jeong, B. Kahng, and D. Kim, Proc. Natl. Acad. Sci. U.S.A. **99**, 12583 (2002); C. P. Herrero, Phys. Rev. E **69**, 067109 (2004).
[21] R. Pastor-Satorras and A. Vespignani, Phys. Rev. Lett. **86**, 3200 (2001); V. M. Eguíluz and K. Klemm, *ibid.* **89**, 108701 (2002).
[22] R. Cohen, D. ben-Avraham, and S. Havlin, Phys. Rev. E **66**, 036113 (2002).
[23] Y. Moreno and A. Vazquez, Europhys. Lett. **57**, 765 (2002).
[24] K.-I. Goh, D.-S. Lee, B. Kahng, and D. Kim, Phys. Rev. Lett. **91**, 148701 (2003).
[25] L. K. Gallos and P. Argyrakis, Phys. Rev. Lett. **92**, 138301 (2004).
[26] M. Catanzaro, M. Boguñá, and R. Pastor-Satorras, Phys. Rev. E **71**, 056104 (2005).
[27] L. K. Gallos and P. Argyrakis, Phys. Rev. E **72**, 017101 (2005).
[28] M. F. Laguna, M. Aldana, H. Larralde, P. E. Parris, and V. M. Kenkre, Phys. Rev. E **72**, 026102 (2005).
[29] G. K. Zipf, *Human Behavior and the Principle of Least Effort* (Addison-Wesley Press, Cambridge, 1949).
[30] M. E. J. Newman, Contemp. Phys. **46**, 323 (2005); N. J. Moura, Jr. and M. B. Ribeiro, Physica A **367**, 441 (2006).
[31] W. Li and X. Cai, Phys. Rev. E **69**, 046106 (2004); R. Guimerá and L. A. N. Amaral, Eur. Phys. J. B **38**, 381 (2004).
[32] J. Ke, Z. Lin, Y. Zheng, X. Chen, and W. Lu, Phys. Rev. Lett. **97**, 028301 (2006).
[33] R. M. Ziff, M. H. Ernst, and E. M. Hendriks, J. Phys. A **16**, 2293 (1983).
[34] Y. Jiang and H. Gang, Phys. Rev. B **39**, 4659 (1989); **40**, 661 (1989).
[35] The data of the populations of all U.S. counties are available at the website http://www.census.gov